

Geometrical configuration and structural response of cable-stayed bridges with curved pylons

Configuración geométrica y respuesta estructural de puentes atirantados con pilonos curvos

Margherita Perona^a, Ana M. Ruiz-Teran^b

^a Master Degree in Civil Engineering, COWI UK Limited, Engineer

mrpo@cowi.com

^b Doctor Ingeniero de Caminos, Canales y Puertos, Imperial College London, Senior Lecturer in Bridge Engineering

a.ruiz-teran@imperial.ac.uk

RESUMEN

Los puentes atirantados son una solución común y eficiente para aplicaciones de gran vano. Se considera que los pilonos curvos, cuya forma es poco convencional, aportan un valor estético adicional al puente, al tiempo que aumentan la complejidad del diseño. Este artículo investiga la respuesta estructural de los puentes con esta disposición, permitiendo la identificación de soluciones de diseño óptimas. Los resultados revelan una excelente respuesta de los puentes seleccionados bajo cargas definidas, validando el proceso de optimización. Además, los análisis de inestabilidad demuestran que la no linealidad geométrica es favorable a la hora de considerar el pandeo del pilono fuera del plano de tirantes.

ABSTRACT

Cable-stayed bridges are a common and efficient solution for long-span applications, widely used in the current practice. Curved pylons, having an unconventional shape, are considered to bring additional aesthetic value to the bridge, whilst increasing the complexity of design. This paper investigates the structural response of bridges with this particular pylon arrangement, allowing the identification of optimal design solutions. The final results reveal an excellent response of the selected bridges under defined loads, validating the optimisation process. In addition, the instability analyses demonstrate that geometrical non-linearities play a favourable role in preventing the buckling of the pylon out of plane.

PALABRAS CLAVE: puente, atirantado, pilono curvo, antifunicular, inestabilidad, no linealidad geométrica

KEYWORDS: bridge, cable-stayed, curved pylon, anti-funicular, instability, geometrical non-linearity

1. Introduction

Cable-stayed bridges are renowned for their excellent capabilities in terms of structural performance, especially when spanning long distances. However, because of the strong visual impact of their superstructure, this type of bridge is often chosen as a mean to achieve an architectural statement. This is the case of cable-stayed bridges with curved pylons, in which the main structural members have been rearranged to achieve a unique aesthetic outcome, however, introducing an additional challenge for the

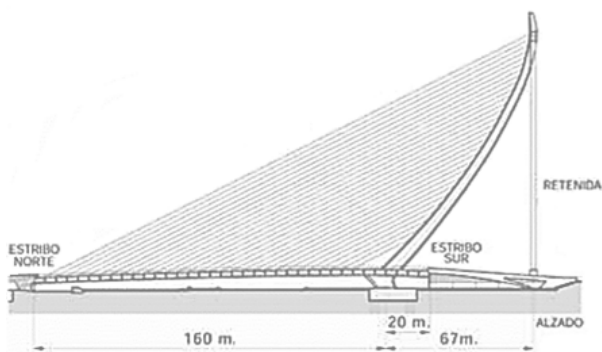
structural design. In fact, the suggestion of an unconventional pylon cancels the benefits of a symmetrical configuration, introducing in the members additional forces, the most relevant of which is the occurrence of bending moments in the pylons.

A relevant example is the Alamillo Bridge (1992), a cable stayed bridge designed by Santiago Calatrava and situated in Seville, Spain. The bridge only has a set of stays towards the main span and aims to counterbalance the forces

from the cables by means of a straight, inclined, stiff and heavy pylon, leaning backwards. Even if highly capturing and innovative, this arrangement is shown to have an inefficient structural form because of the very high bending moments introduced in the pylon, and a clear indication of this is the extreme weight of this member compared with other bridges of the same type [1].

Guest et al. [1] presented a good comparison between the Alamillo Bridge and the Erasmus Bridge in Rotterdam, which incorporates a single pair of backstays to provide the necessary restoring force. This addition does not considerably affect the aesthetics but has a substantial influence on the pylon's section. In fact, as presented by De Jong and Annema [2], the Erasmus Bridge's pylon resulted to be around ten times lighter than the one of the Alamillo Bridge.

According to this evidence, a set of forestays anchored to a single shaped pylon, provided with some backstays, is proved to be a more reasonable and attainable solution. A few structures with this configuration have been proposed by Calatrava during the following years, such as the Káthaki Bridge (2004) [3] in Athens, the Serrería Bridge (2008) [4] in Valencia and the Samuel Beckett Bridge (2009) [5] in Dublin. These three structures, very similar to each other in structural arrangement, have been used as a basis for the literature review which supports this paper. An elevation of the Serrería Bridge is shown in Figure 1 for reference.



Elevation of the Serrería Bridge [4]

2. Definition of anti-funicular pylon shapes

Whilst the asymmetrical configuration of the cables introduces additional forces in the members, the introduction of a curvature in the pylon's shape enables the optimisation of the structural performance through design. In fact, given a fixed loading condition, it is possible to obtain the shape of the pylon which minimises the bending moments and allows the tower to work mainly under compression, i.e. the anti-funicular shape of that particular loading. In this section, the analytical and numerical procedure developed to calculate this shape are illustrated.

2.1 Analytical equation

Based on the geometry of existing bridges of this kind, a simplified model for a generic cable-stayed bridge with a curved pylon has been developed for the purpose of this calculation and a graphical representation is shown in Figure 2. The following quantities are assumed to be known:

- L Length of the main span of the bridge [m]
- L_0 Length of the back span of the bridge [m]
- α Inclination of the forestays – identical for every cable [°]
- γ Inclination of the backstay [°]
- s Horizontal spacing between the forestays [m]

From geometry, the height of the pylon H is determined accordingly.

To express the position of the points of the pylon, a non-orthogonal reference system is introduced, in which the coordinates are expressed as follows:

- x Distance from a point (x,y) on the pylon to the backstay [m]
- y Distance from a point (x,y) on the pylon to the top forestay [m]

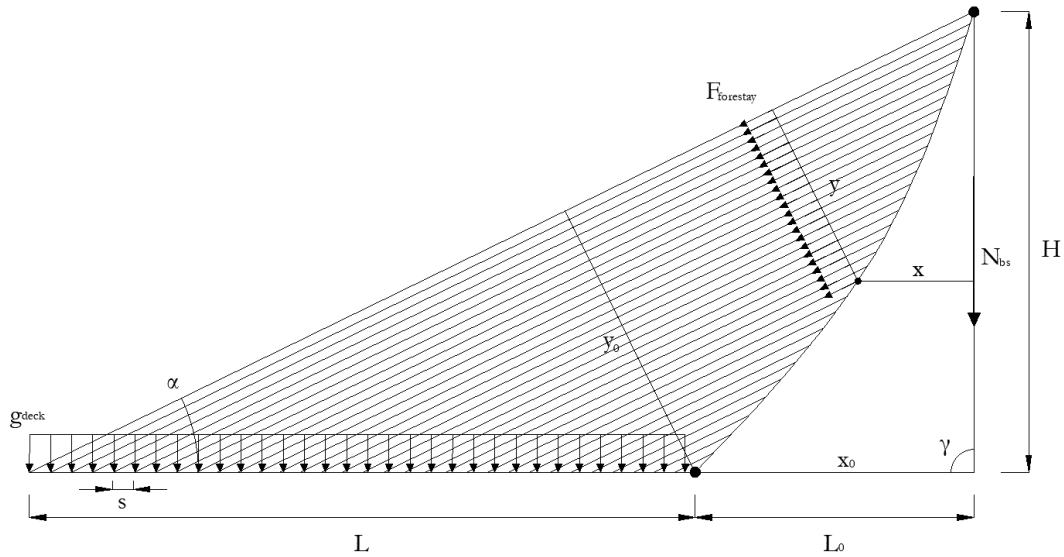


Figure 2: Visual representation of bridge model used to determine anti-funicular pylon shapes

The origin of the system is located at the tip of the pylon and, based on the given geometry, the base of the pylon is fixed and is identified by the coordinates (x_0, y_0) .

Since the shape of the pylon can be anti-funicular just under a specific loading condition, a fixed uniformly distributed load g_{deck} is taken into consideration at this stage and applied on the main span of the bridge. If the cables have been pre-stressed to cancel out the vertical displacements in the deck under permanent load, the axial force in every forestay, F_{fs} , can be determined. Imposing the condition of nil bending moment at the base of the pylon, the restoring force required in the backstay, N_{bs} , is calculated through Equation 1. Subsequently, the same condition can be imposed to every generic point of the pylon, identified by the coordinates (x, y) , leading to Equation 2. The set of coordinates which satisfies this equation represents the points at which the bending moment is zero: therefore, the equation represents the analytical expression of the anti-funicular shape of the pylon.

$$N_{bs} = \frac{g_{deck} L^2}{2x_0} \quad (1)$$

$$x = \frac{g_{deck}}{2 \sin^2 \alpha N_{bs}} y^2 \quad (2)$$

Nevertheless, it has to be noted that this procedure cannot take into account the self-weight of the pylon, as the effect of this force depends on the shape of the pylon itself, which is still unknown at this stage. Therefore, this is applicable just in cases in which this load is negligible or when the pylon wants to be shaped as anti-funicular of a uniformly distributed loading. For this reason, in cases in which the weight of the pylon has to be taken into account, the employment of a numerical procedure is necessary.

2.2 Numerical procedure

For the purpose of this calculation, the length of the pylon is discretised and its shape is calculated as a set of coordinates, each one corresponding to a section of pylon, with a defined length and area. To allow for different modellings of the pylon's weight, the area can be defined as a function of the position, with a defined rate of variation of the cross-section along its length.

As a preliminary shape, the one obtained neglecting the self-weight of the pylon is considered. The initial set of coordinates can

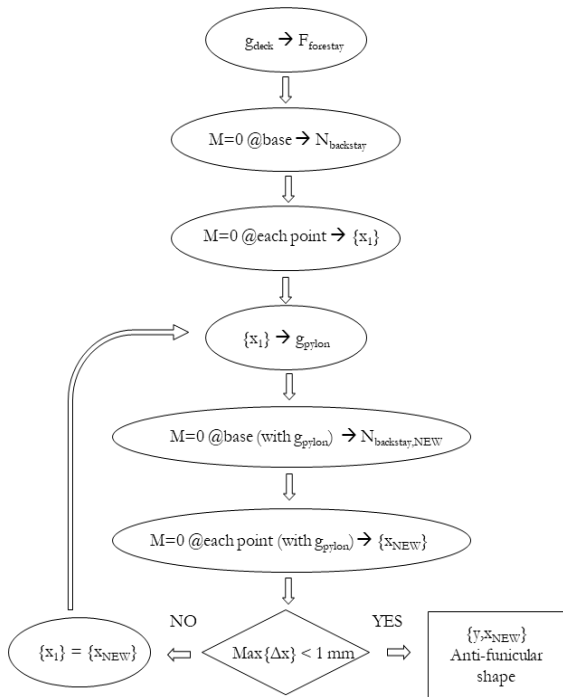


Figure 3: Numerical procedure for the calculation of the anti-funicular shape of the pylon

now be used to determine the self-weight forces and to determine the new anti-funicular shape accordingly. Nevertheless, the procedure at this stage will not give an exact result, because the self-weight forces are obtained based on the previous shape of the pylon and not on the current one, which is still unknown. For this reason, an iterative process is followed until the changes on the x coordinate are smaller than a determined value (1mm for this study). The procedure is summarised in the flowchart in Figure 3.

3. Parametric studies to define optimal geometrical configurations

In order to identify which structural configurations perform better, a parametric analysis is conducted varying several geometric properties of the structure and considering their influence and effect on the pylon's anti-funicular shape, the bridge geometry and the structural performance of the bridge. At this stage, the dead load on the deck, the prestressing of the

cables and the self-weight of the pylon have been applied. The following parameters have been considered:

- α Inclination of the forestays – set to a constant value of 20° throughout the study;
- γ Inclination of the backstay – varied from a minimum of 10° to a maximum of 110° ;
- $\frac{L_0}{L}$ Spans' ratio – for constant values of the main span L , the length of the back span L_0 has been varied to get values of the ratio ranging from 0.2 to 0.5 (higher values were not explored, considering that the back span is significantly smaller than the main span for this configuration).

The impact of the parameters above has been assessed on the following non-dimensional quantities:

- $\frac{N_{pylon,base}}{g_{deck}L}$ Ratio between the axial force at the base of the pylon and the dead load on the deck;
- $\frac{N_{backstay}}{g_{deck}L}$ Ratio between the axial force required in the backstay and the dead load on the deck;
- $\frac{H}{L}$ Ratio between the height of the pylon and the length of the main span;
- $\frac{L_{forestays}}{L}$ Ratio between the total length of forestays required and the length of the main span of the deck.

3.1 Analysis of results

As the results of the analysis revealed very similar trends for all the values of the spans' ratio L_0/L , only the results corresponding to a fixed

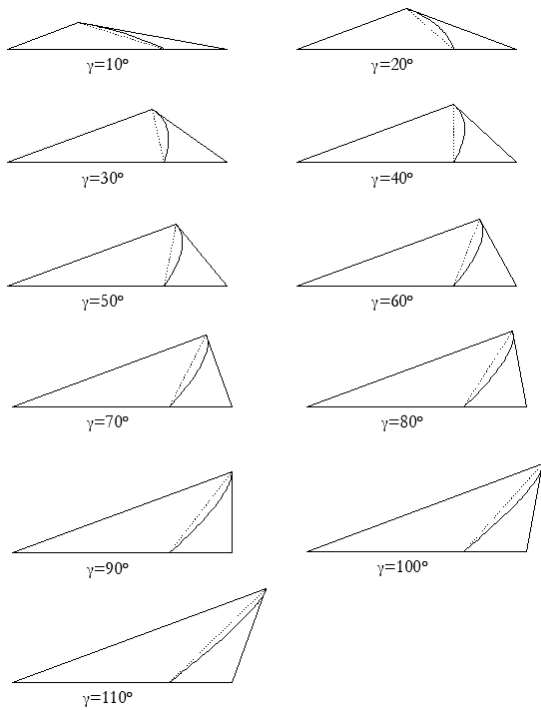


Figure 4: Anti-funicular shapes of the pylon for different values of inclination of the backstay ($L_0/L=0.4$)

condition of $L_0/L=0.4$ are shown and discussed in the following.

To analyse the evolution of the anti-funicular shapes, the geometric configurations obtained for the different values of γ are shown in Figure 4. Whilst for small and big values of the inclination of the backstay the anti-funicular shape looks reasonably shallow (with very limited curvature), a much bigger deviation from the straight alignment of the pylon is observed for intermediate values of the angle, where a more capturing aesthetic effect is achieved.

As it can be observed in Figure 5(b), the axial force at the base of the pylon and the one required in the backstay are strictly related and follow a similar pattern with γ . In fact, since the backstay plays a relevant role in the determination of the resultant force in the tower, their trends can be explained focusing on the force in the backstay. For smaller values of γ , the anti-funicular pylon is leaning completely towards the main span and therefore the self-weight represents an additional component to be counterbalanced by the backstay, in which very large forces would be required. As the angle

raises, the pylon becomes a more stabilising component to the equilibrium, reducing dramatically the force required in the backstay.

In terms of final geometry, the graphs in Figure 5 show that both the height and the total lengths of forestays required increase with γ , as a result of the overall geometrical configuration of the bridge.

To summarise, it can be stated that:

- the required force in the backstay and, accordingly, the axial force at the base of the pylon are unreasonably high for values of γ below 30° and in particular for 10° . The amount of material required for these two elements would grow significantly, which would have important implications on the cost;
- the height of the pylon is close to the optimal value for cable-stayed bridges $H=0.36L$ (which is equivalent to a minimum angle of the stay cables of 20°) with values of γ between 30° and 60° ;
- the total length of forestays needed grows dramatically with γ - the lengths of

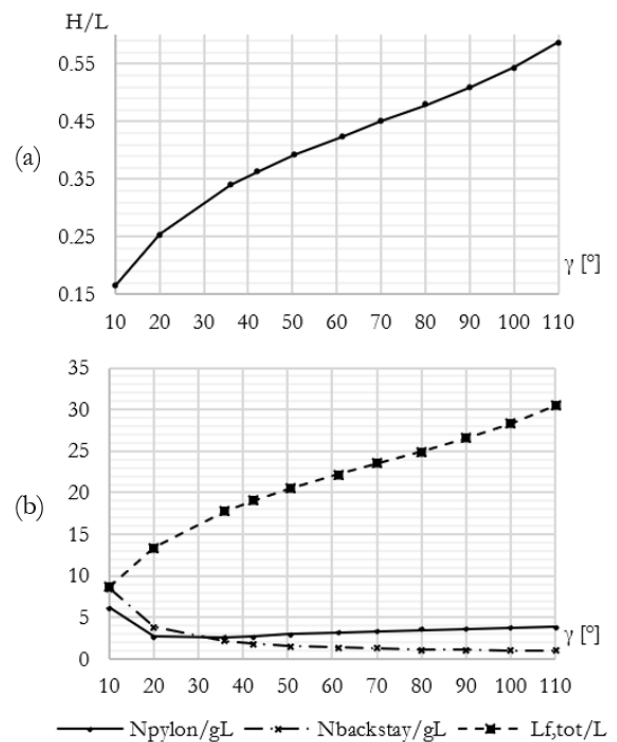


Figure 5: Investigated values with the inclination of the backstay γ : (a) H/L , (b) Forces ratios (N_{pylon}/gL , $N_{backstay}/gL$), and $L_{f,tot}/L$ ratio

forestays necessary with $\gamma=110^\circ$ are more than double the ones required with $\gamma=20^\circ$;

- the visual effect of a rounded shape is emphasised for values of γ between 20° and 80° .

3.2 Selection of cases to be further analysed

In view of the considerations made in the previous section, it can be stated that the best results in term of visual effect, magnitude of the forces and amount of material employed are obtained with values of γ between 30° and 60° .

In order to determine a combination of parameters for an optimal bridge geometry to be examined more in detail, the height of the pylon has been taken into consideration. As mentioned above, a recommended value of H/L for cable-stayed bridges with a single pylon is 0.36 and this can be obtained, with a ratio between the lengths $L_0/L=0.4$, for a value of $\gamma=40^\circ$.

In addition to this optimal geometry, two more bridges are selected, to compare the performance of this arrangement to those with more extreme configurations. Keeping unvaried the lengths' ratios to 0.4, the ratio H/L is chosen equal to 0.25 and 0.5, leading to, respectively, $\gamma=20^\circ$ and $\gamma=90^\circ$.

4. Validation through FE analysis

In this section, the three bridges selected previously are subjected to finite element analysis in order to investigate more thoroughly their structural response under permanent and live load and validate the results of the numerical and the parametric analyses.

4.1 Finite elements models

The three bridges are modelled consistently with the geometric assumptions made in Section 2. The flat deck is divided into a main span, on the

left of the pylon, and a back span on the right. The forestays are equally distributed along the whole length of the main span with a spacing of 5 meters and are arranged in a harp system with an angle α of 20° . A single backstay connects the tip of the pylon with the right end of the back span, with an inclination of 20° , 40° and 90° for Case 1, 2 and 3 respectively. The shapes of the pylons are the anti-funicular one corresponding to each set of parameters.

The section properties of the members are determined based on a database built from a literature review of existing bridges of this kind. However, simplified versions of these are assumed for the purpose of this study. The cross-section of the deck is composed by a central steel box girder with sideways cantilevers. The steel plates composing the cantilevered flanges have a thickness of 14 mm, while the webs and the flanges of the central girder are respectively 22 and 30 mm thick. The pylon's section is made of a steel rectangular box, in which the thickness of all the members is 60 mm; the section is oriented with the short side facing the main span of the deck. Both sections are uniform along the length of the elements.

In terms of the cables, all the forestays have a cross sectional area of 7800 mm^2 , while the backstay's section vary depending on the model case. An area of 31500 mm^2 is chosen for Case 1 because, from the results analysed in Section 3.1, the backstay is expected to carry larger forces. In Case 2 and 3 instead the area of the backstay is reduced to 17600 mm^2 . For this analysis, all the anchorages of the cables are considered to be located at the centroids of both the deck and the pylon's sections.

4.2. Permanent loading condition

In this section, the behaviour of the described bridges is analysed under permanent loads. This includes the distributed dead load on the deck (145 kN/m), the self-weight of the pylon (75 kN/m) and the pre-stressing of the cables, appropriately calculated.

It is important to highlight that the bridges are behaving as expected. Deflections along the deck are negligible and the bending moment diagrams, resembling the ones of continuous beams with supports where the deck is supported by the stay cables, suggest a correct behaviour of the pre-stressing system. Regarding the pylons, the maximum bending moment values are experienced at the base. Comparing them with the values of the axial force at the same location, the eccentricities are obtained. These are of the magnitude of a few millimetres, negligible if compared to the pylon's sections, which confirms that the shapes of the towers are, effectively, anti-funicular. The results of this analysis are shown in Figure 6 and summarised in Table 1.

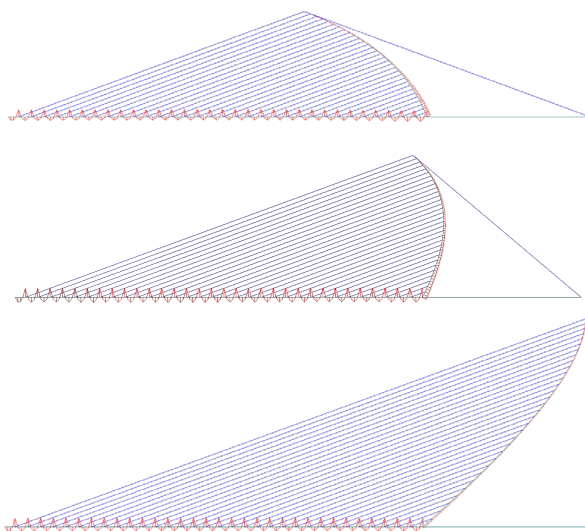


Figure 6: Bending moment diagrams under permanent loads for model case 1, 2 and 3 respectively

4.3. Live loading condition

In this section, the response of the structures is examined by means of a linear analysis under an additional live load $q=100$ kN/m uniformly distributed along the length of the main span. The bending moment diagrams are shown in Figure 7. The outputs of the analysis are summarised in Table 1.

The shape chosen is not anti-funicular of a uniformly distributed load, as it included also the weight of the pylon and the prestressing of the stay-cables in addition to the uniformly distributed weight of the deck. For this reason, significant bending moments appear now both on the deck and the pylon. In fact, even the smallest among the values observed at the base of the pylon, which occurs in Case 3, corresponds to an eccentricity of 1.1 m, which is significant. Furthermore, the prestressing system has been designed to cancel the vertical displacements of the deck under the permanent loads only. Therefore, the behaviour of the deck under additional loads is the same one that a cable-stayed bridge would experience under dead load when the cables have not been prestressed.

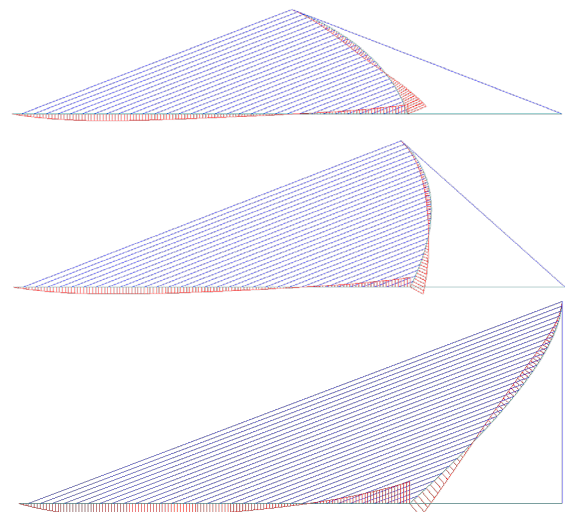


Figure 7: Bending moment diagrams under permanent and live loading condition for model case 1, 2 and 3 respectively

Table 1: Bending moment and eccentricity values under permanent (PL) and live load (LL) conditions

Case	$M_{\max, \text{deck}}$ (kNm)	$M_{\text{pylon, base}}$ (kNm)	$e_{\text{pylon, base}}$ (m)
1 (PL)	325	170	0.0027
2 (PL)	310	138	0.0022
3 (PL)	307	48	0.0006
1 (PL+LL)	119500	275200	4.2
2 (PL+LL)	131200	206000	2.6
3 (PL+LL)	147800	117800	1.1

5. Instability

Considering that the pylon member in these arrangements is subjected to large compression forces, two types of instability analysis are carried out in order to assess the potential buckling of the pylon.

5.1. Elastic buckling analysis

A modal buckling analysis is carried out. During this type of analysis, the software increments the defined set of loads by a factor λ , until reaching the different buckling modes of the structure. The first buckling mode is the one of interest in this case.

While carrying out the analysis, the software increments all the defined loads by the same factor λ at the same time. This does not reflect the real situation, as it is not realistic to expect that the prestressing increases, whereas the permanent or live loads can increase. For this reason, two different analyses are conducted for each model case: one in which the structure is subjected to all the permanent and live loads (condition A) and one in which the only live load is applied (condition B). Despite of the simplification, condition A is more realistic, as it includes the compression forces in the pylon due to permanent loads, which are not considered in condition B. This allows to calculate two values of the factor λ , λ_A and λ_B , which represent respectively a lower and upper bound for the real load factor. For Case 1 the load factors in conditions A and B are respectively 5 and 48. For Case 2, which shows the best performance, $\lambda_A=11$ and $\lambda_B=55$, while for Case 3 $\lambda_A=7$ and $\lambda_B=38$. The analysis also highlighted that the first mode always involves the buckling of the pylon out of plane.

5.2. Geometric non-linear analysis

In order to investigate more accurately the instability of the pylons, an additional geometrical non-linear analysis is carried out.

In this case, to obtain the buckling of the pylon out of the plane, initial imperfections have to be modelled in the pylon's shape. The three models are then modified imposing, as initial profile of the pylon, the deformed shape of the first correspondent buckling mode obtained through elastic analysis, properly scaled. The sensitivity of the analysis to the magnitude of the initial imperfections at the top of the pylon has been assessed between values of 10 and 500 mm and found to be negligible for the purpose of determining the final buckling load. Imperfections are then modelled so that the tip of the pylon is displaced by $\delta_0 = 100$ mm in the undeformed condition. With this initial geometry, a set of non-linear analysis is carried out, monitoring the lateral displacement of the top of the pylon while incrementing the value of the only live load. The results for Cases 1, 2 and 3 are presented in Figure 8.

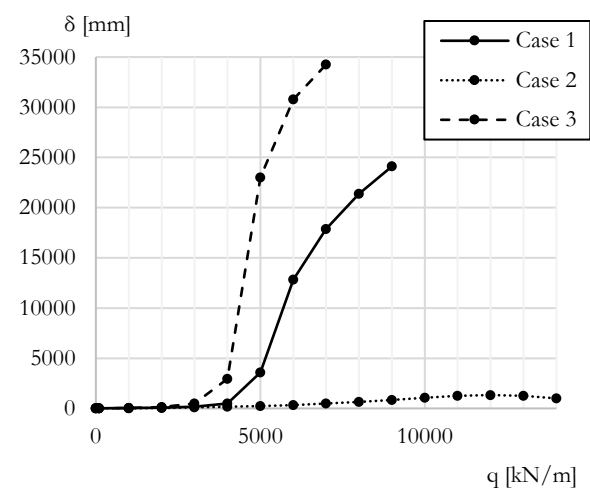


Figure 8: Displacements of the top of the pylon out of plane for increasing values of the live load

Comparing these results with the one obtained from the elastic buckling analysis, the live load factors appear considerably higher. In fact, calling q_{EBA} the buckling live load calculated from the elastic buckling analysis and q_{NLA} the one obtained in the non-linear case, the following ratios can be calculated:

- Case 1: $q_{NLA}/q_{EBA}=1.875$
- Case 2: $q_{NLA}/q_{EBA}=2.18$
- Case 3: $q_{NLA}/q_{EBA}=1.84$

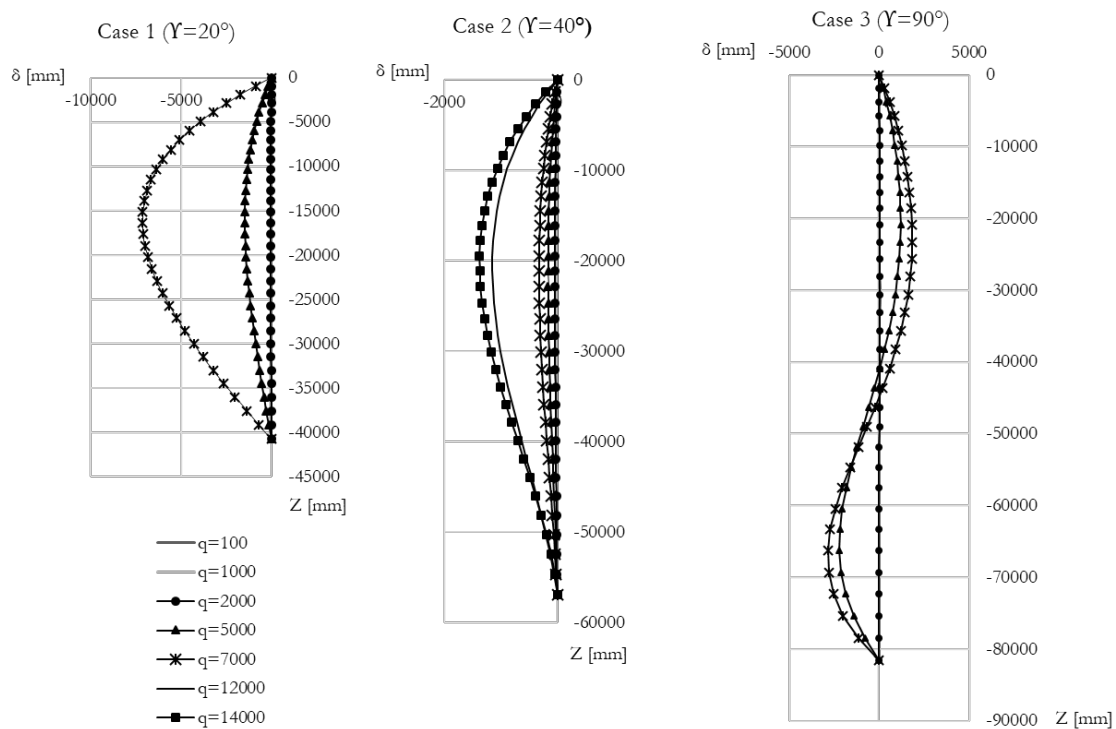


Figure 9: Lateral displacement of pylon from straight inclined alignment for increasing values of the live load cases 1, 2 and 3 respectively

These results can be justified considering the interaction of the pylon with the cable-stayed system. As the top of the pylon displaces laterally, the cable is now inclined and its force has a horizontal restoring component which acts to pull the pylon back towards the initial position. At the same time, the forces induced by the cables make the pylon behave as a pinned column, and not as a cantilever with a free end. If the cables were arranged in a pure fan system, the buckling length of the tower would be very similar to the pylon's height, which is half of the free cantilever [6]. Even if, in these cases, the arrangement of the cables is a harp system, the condition of the pylon can still be considered as the one of a pinned column. The tower is subjected to a distributed loading instead of a concentrated force at the top, but the only two points of the pylon in which the bending moment is equal to zero are the top and the base, which represent indeed the pins. This is an acceptable assumption when the lateral rigidity of the deck is large enough to restrain the lateral displacement of the section where the stay cables are anchored to the deck.

A confirmation of this behaviour can be found analysing the deformed shape of the whole column. Analysing, in fact, the lateral bending of the pylon with respect to its straight alignment (Figure 9) it is clear that the pylon is actually buckling as a pinned column, because the amplitude of the curves is increasing with the live load until the buckling point. It can also be observed that the profile assumed by the buckling shapes is reflecting, in each case, the first buckling mode shape, which is a natural consequence of the chosen way of modelling the initial imperfections.

This evidence about the instability behaviour of the pylon justifies the higher values of the buckling load obtained with a geometric non-linear analysis. It is worth highlighting that the higher coefficient is obtained for Case 2, which is the actual optimal geometrical configuration selected on the base of the previous studies conducted in this paper.

The employment of a geometrical non-linear analysis is then crucial in the study of the instability of the pylon out of plane. In fact, the non-linear analysis accounts for the deformed

shape in the resolution of the structure, giving rise to the beneficial effect mentioned above. In the elastic buckling analysis instead, the deformation of the pylon is not taken into account. This does not allow the system to benefit from the favourable restoring effects and, consequently, leads to the calculation of lower buckling loads, based only on the magnitude of the compressive forces in the pylon.

6. Conclusions

With regards to the curved geometry of the pylon, the paper presents an analytical formulation that allows to obtain the anti-funicular shape of the pylon under a uniformly distributed load applied on the deck, when the stay cables are prestressed and the weight of the pylon is neglected, which is useful for preliminary design. In addition, an effective and accurate numerical procedure is developed to account for the weight of the pylon as well. With a view to design, a reasonable solution would be to optimise the performance of the bridge under quasi-permanent live load, so that a reasonable portion of the effects of the loads could be taken into account and mitigated.

The results of the instability analyses also highlight the necessity of considering geometrical non-linearities. The cable-stayed system, in fact, represents a significant favourable contribution to the resistance of the pylon in buckling out of plane and this is not taken into account with an elastic modal buckling analysis.

In addition, the instability analyses give a further evidence of the better behaviour, among the modelled cases, of the bridge which was selected as the optimal one for design purposes. This is a further confirmation of the relevance and the utility of the parametric analysis, according to which optimal performances, in terms of structural behaviour and aesthetic design, are obtained for this kind of bridge when

the inclination of the backstay takes values between 30° and 60° .

In conclusion, the paper illustrates a set of measures which can be taken, through the design of a cable-stayed bridge with a curved pylon, to optimise the performance of the structure in service.

Acknowledgements

The author is heartily thankful to the supervisor of this project, Dr. Ana M. Ruiz-Teran, for her strong guidance and encouragement throughout the months spent at Imperial College London.

References

- [1] J.K. Guest, P. Draper, D.P. Billington, Santiago Calatrava's Alamillo Bridge and the Idea of the Structural Engineer as Artist, *Journal of Bridge Engineering*. 18 (2013), 936-945.
<https://ascelibrary.org/doi/full/10.1061/%28ASCE%29BE.1943-5592.0000445>
- [2] M. De Jong, J.A. Annema, The Erasmus Bridge: Success factors according to those involved in the project (2008). Available from: <http://resolver.tudelft.nl/uuid:e2f9a163-5471-4bb0-9071-fce5df43ed90>
- [3] S. Calatrava, Katchaki Pedestrian Bridge. Available from: <https://calatrava.com/projects/katchaki-pedestrian-bridge-athens.html>
- [4] S. Calatrava, Serrería Bridge. Available from: <https://calatrava.com/projects/serreria-bridge-valencia.html>
- [5] J. Cutter, J.W. Flanagan, P. Brown, M. Rando, G. Mo, Samuel Beckett Bridge, Dublin, Ireland. *Bridge Engineering*. 164 (2011), 133-144.
- [6] ESDEP WG 14, Section 15B.8: Cable-stayed bridges, 1995